Multiband effects and possible Dirac states in $LaAgSb_2$

Kefeng Wang (王克锋) and C. Petrovic
Condensed Matter Physics and Materials Science Department, Brookhaven National Laboratory, Upton, New York 11973, USA
(Received 13 July 2012; revised manuscript received 4 September 2012; published 25 October 2012)

Here, we report the possible signature of Dirac fermions in the magnetoresistance, Hall resistivity, and magnetothermopower of $LaAgSb_2$. The opposite sign between the Hall resistivity and Seebeck coefficient indicates the multiband effect. Electronic-structure calculations reveal the existence of the linear bands and the parabolic bands crossing the Fermi level. The large linear magnetoresistance was attributed to the quantum limit of the possible Dirac fermions or the breakdown of weak-field magnetotransport at the charge-density-wave phase transition. Analysis of Hall resistivity using a two-band model reveals that Dirac holes which dominate the electronic transport have much higher mobility and larger density than conventional electrons. The magnetic field suppresses the apparent Hall carrier density, and also induces the sign change of the Seebeck coefficient from negative to positive. These effects are possibly attributed to the magnetic field suppression of the density of states at the Fermi level originating from the quantum limit of the possible Dirac holes.

DOI: 10.1103/PhysRevB.86.155213 PACS number(s): 75.47.Np, 72.20.Pa, 72.80.Ga

I. INTRODUCTION

Recently, layered rare-earth antimonides have been attracting wide attention due to their possible relationship to superconductivity, charge density wave (CDW), and colossal magnetoresistance (MR).[1–4] For example, two-dimensional (2D) superconductivity ($T_c \sim 1.7$ K) was observed in $LaSb_2$ under ambient pressure, while application of hydrostatic pressure induces a two- to three-dimensional superconducting crossover.[2,3] Large positive magnetoresistance was observed in $LaSb_2$ and $LaAgSb_2$.[3–7] $LaSb_2$ exhibits a large linear magnetoresistance with no sign of saturation up to 45-T fields and $[\rho(H) - \rho(0)]/\rho(0) \sim 10^4\%$.[4] MR in $LaAgSb_2$ is also linear and reaches ~2500% in an 18-T field.[6] The resistivity of $LaAgSb_2$ exhibits a significant anomaly at ~210 K which was attributed to the possible CDW transition.[6,7] Very large magnetothermopower effects were observed in $LaAgSb_2$.[9] The magnetoresistance and magnetothermopower effects in these materials are extraordinary and are still poorly understood. This is because the semiclassical transport in conventional metals gives quadratic field-dependent MR in the low-field range, which would saturate in the high field, and the diffusive Seebeck coefficient does not depend on the external magnetic field.[10]

Large linear MR was also observed recently in $SrMnBi_2$, which has similar crystal structure to $LaAgSb_2$.[11–13] The crystal structure of $SrMnBi_2$ contains alternatively stacked MnBi layers and two-dimensional Bi square nets separated by Sr atoms along the c axis.[11,12] Highly anisotropic Dirac states were identified in $SrMnBi_2$ where linear energy dispersion originates from the crossing of two Bi $6p_{x,y}$ bands in the double-sized Bi square net.[11] The linear MR is attributed to the quantum limit of the Dirac fermions.[11,13,14] In high enough field, the electronic systems enter the extreme quantum limit where all of the carriers occupy only the lowest Landau level (LL) and a large linear MR could be expected.[14,15] Unlike the conventional electron gas with parabolic energy dispersion, the distance between the lowest and first LLs of Dirac fermions in a magnetic field is very large and the quantum limit is easily realized in the low-field region.[16,17] Consequently, some quantum transport phenomena such as quantum Hall effect and large linear MR could be observed in the low-field region for Dirac fermion materials such as graphene,[16,17] topological insulators,[18–20] $Ag_{2-\delta}Te/Se$,[21–23] iron-based superconductors $BaFe_2As_2$,[24,25] and La(Fe,Ru)AsO,[26] as well as $SrMnBi_2$.[11,13]

In this paper, we attribute the large linear magnetoresistance and magnetothermopower in $LaAgSb_2$ to the quantum limit of Dirac fermions as revealed by *ab initio* calculation, or to the breakdown of weak-field magnetotransport at the CDW phase transition. Interestingly, the Hall resistivity is positive, but the Seebeck coefficient is negative in the 0-T field. Analysis of Hall resistivity using a two-band model reveals that Dirac holes have higher mobility and larger density than conventional electrons, and dominate the electronic transport. The magnetic field suppresses the apparent Hall carrier density, and also induces the sign change of the Seebeck coefficient from negative to positive. These effects are attributed to the magnetic field suppression of the density of states at the Fermi level originating from the quantum limit of the Dirac holes.

II. EXPERIMENT

Single crystals of $LaAgSb_2$ were grown using a high-temperature self-flux method.[6] The resultant crystals are platelike. X-ray diffraction (XRD) data were taken with Cu K_α ($\lambda = 0.15418$ nm) radiation of a Rigaku Miniflex powder diffractometer. Electrical transport measurements up to 9 T were conducted in Quantum Design PPMS-9 with the conventional four-wire method. In the in-plane measurements, the current path was in the ab plane, whereas magnetic field was parallel to the c axis. Thermal transport properties were measured in Quantum Design PPMS-9 from 2 to 350 K using a one-heater–two-thermometer method. The direction of heat and electric current transport was along the ab plane of single grain crystals with magnetic field along the c axis and perpendicular to the heat/electrical current. The relative error in our measurement was $\frac{\Delta\kappa}{\kappa} \sim 5\%$ and $\frac{\Delta S}{S} \sim 5\%$ based on Ni standard measured under identical conditions. First-principles electronic-structure calculations were performed using experimental lattice parameters within the full-potential linearized augmented plane-wave (LAPW)

method[27] implemented in the WIEN2K package.[28] The general gradient approximation (GGA) of Perdew *et al.* was used for the exchange-correlation potential.[29]

III. RESULTS AND DISCUSSIONS

The crystal structure of $LaAgSb_2$ [Fig. 1(a)] features La ions between alternatively stacked two-dimensional Sb layers (red balls) and AgSb layers along the c axis. The first-principles electronic-structure calculations reveal that the density of states (DOS) at the Fermi level is very small [Fig. 1(b)] and is dominated by the states coming from two-dimensional Sb layers. There are three nearly linear narrow bands crossing the Fermi level along $Z-A$, $Z-R$, and $\Gamma-M$ directions, respectively [as indicated by the red circles in Fig. 1(c)]. Because of the occupation of Ag ions below and above the quasi-two-dimensional Sb layers, the unit cell of Sb layer has two Sb atoms [Fig. 1(a)]. This will lead to the folding of the dispersive p orbital of Sb. The two $p_{x,y}$ bands from two Sb

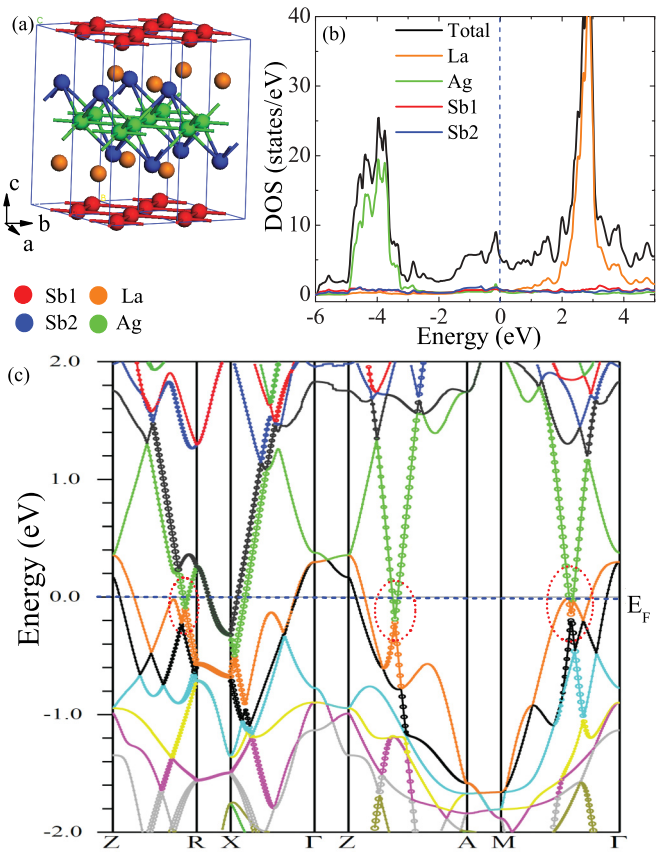

FIG. 1. (Color online) (a) The crystal structure of $LaAgSb_2$. Sb atoms in 2D square nets (Sb1) are shown by red balls. Ag atoms are denoted by green balls. Sb atoms in $AgSb_4$ tetrahedrons (Sb2) are denoted by blue balls. La atoms are denoted by orange balls. Blue lines define the unit cell. (c) The total density of states (DOS) (black line) and local DOS from La, Ag, Sb1, and Sb2 in $LaAgSb_2$. The dotted line indicates the position of the Fermi energy. (d) The band structure for $LaAgSb_2$. The lines with open circles indicate the bands with $p_{x,y}$ character. The line at energy = 0 indicates the position of the Fermi level and the red circles indicate the position of Dirac-cone-like points.

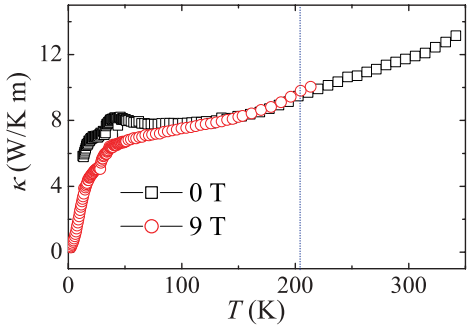

FIG. 2. (Color online) In-plane thermal conductivity $\kappa(T)$ of $LaAgSb_2$ single crystal as a function of temperature in 0- and 9-T magnetic fields, respectively. The blue line indicates the sharp anomaly at ~210 K.

atoms cross each other at a single point and then form the nearly linear band and Dirac-cone-like point around the Fermi level [Fig. 1(c)]. This is similar to the case of $SrMnBi_2$ where the crossing of Bi $6p_{x,y}$ orbitals forms the Dirac-cone-like point.[11]

Powder x-ray diffraction results confirmed phase purity of our crystals, and the temperature- and magnetic-field-dependent resistivity and Seebeck coefficient agree very well with previous reports.[6–9] Figure 2 shows the thermal conductivity κ in 0- and 9-T magnetic fields perpendicular to the ab plane. The thermal conductivity κ exhibits a CDW anomaly at about 210 K (blue dashed line) that corresponds to similar anomalies in $\rho(T)$ and $S(T)$ already reported in literature.[6,7,9] It is suppressed significantly by the magnetic field below 200 K (Fig. 2).

$LaAgSb_2$ exhibits very large linear magnetoresistance. Below 30 K, the in-plane magnetoresistance $MR = [\rho_{ab}(B) - \rho_{ab}(0)]/\rho_{ab}(0)$ exhibits a sharp dip at low field and then increases nearly linearly with increasing field at higher field (>1 T), as shown in Fig. 3(a). At higher temperature (>40 K), the dip at low field disappears [Figs. 4(a) and 4(b)]. Below

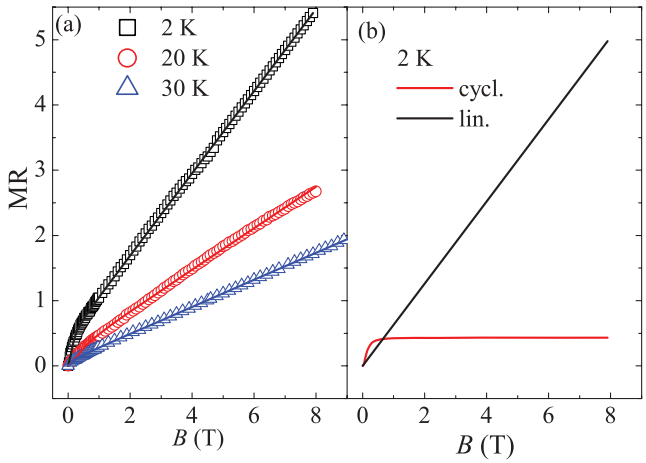

FIG. 3. (Color online) (a) The magnetic field (B) dependence of the in-plane magnetoresistance MR at different temperatures from 2 to 30 K. The open symbols are the experimental data and solid lines are the fitting results using Eq. (3). (b) The linear and cyclotronic contributions to the magnetoresistance at 2 K derived from fitting using Eq. (3).

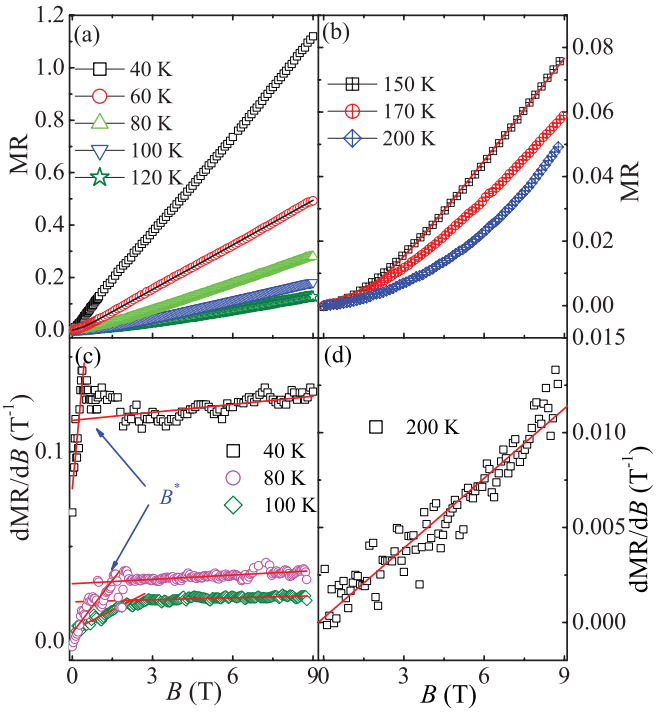

FIG. 4. (Color online) (a), (b) The magnetic field (B) dependence of the in-plane magnetoresistance (MR) at different temperatures above 40 K. (c), (d) The field derivative of in-plane MR, d MR/dB, as a function of field (B) at different temperatures, respectively. The red lines in the high-field regions were fitting results using MR = $A_1B + O(B^2)$ and the lines in low-field regions using MR = A_2B^2.

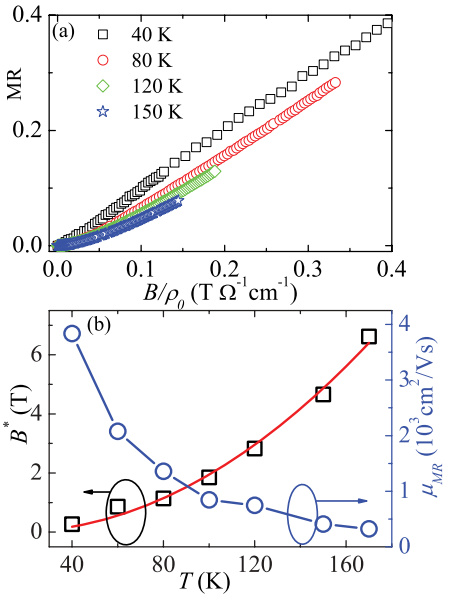

FIG. 5. (Color online) (a) The Kohler's plots for MR at different temperatures. (b) Temperature dependence of the critical field B^* (black squares) and the effective MR mobility $\mu_{\rm MR}$ (blue circles) extracted from the weak-field MR. The red solid line is the fitting result of B^* using $B^* = \frac{1}{2e\hbar v_F^2}(E_F + k_BT)^2$.

1 T at 2 K, dMR/dB is proportional to B [as shown by lines in low-field regions in Fig. 4(c)], indicating the semiclassical quadratic field-dependent MR ($\sim A_2B^2$). But, above a characteristic field B^*, dMR/dB deviates from the semiclassical behavior and saturates to a much reduced slope [as shown by lines in the high-field region in Fig. 4(c)]. This indicates that the MR for $B > B^*$ is dominated by a linear field dependence plus a very small quadratic term [MR $= A_1B + O(B^2)$]. With increasing temperature, the magnetoresistance is gradually suppressed and the crossover field B^* increases rapidly [Fig. 4(a)]. Above 200 K, linear MR becomes invisible in our magnetic field range ($0 \sim 9$ T) [Fig. 4(b)] and the MR in the whole field range is quadratic [Fig. 4(d)].

Single-band semiclassical transport gives that magnetoresistance scales as MR $= f(B\tau) = F(B/\rho_0)$ with the assumption of the single scattering time τ, i.e., $1/\tau(T) \propto \rho_0(T)$, where $\rho_0(T)$ is the zero-field resistivity.[10,30] The linear unsaturated magnetoresistance of $LaAgSb_2$ clearly deviates from semiclassical transport and also violates Kohler's scaling, particularly in the high-field region [Fig. 5(a)], indicating multiband or quantum effects.

In metals with two types of carriers (holes and electrons), semiclassical transport and the cyclotronic motion gives

$$\frac{\rho(H) - \rho(0)}{\rho(0)} = \frac{\sigma_h\sigma_e(\mu_h + \mu_e)B^2}{(\sigma_h + \sigma_e)^2 + (\sigma_h\mu_e + \sigma_e\mu_h)^2B^2}, \qquad (1)$$

where σ_e (σ_h) and μ_e (μ_h) are the electronic conductivity and mobility for electrons (holes), respectively. This formula usually results in the quadratic field-dependent MR in the low-field range and saturated MR in the high field.[10,26]

Hitherto, there are several possible mechanisms for linear MR. In the single crystal with open Fermi surface (such as the quasi-one-dimensional Fermi surface sheet), along the open orbits there will be B^2-dependent MR in very high field. The linear MR might also be observed in the polycrystalline sample due to average effect.[10,14] This mechanism obviously does not attribute to our results since our sample is a high-quality single crystal. Linear MR could also arise due to the quantum limit in the high magnetic field.[14,15] Application of strong magnetic field (B) results in quantized Landau levels E_n (LLs). When the field is very large and the difference between the zeroth and first Landau levels $\triangle_{\rm LL}$ exceeds the Fermi energy E_F and the thermal fluctuation k_BT, all carriers only occupy the lowest LL and a large linear MR could be expected:

$$\text{MR} = \frac{1}{2\pi}\left(\frac{e^2}{\varepsilon_\infty\hbar v_F}\right)^2\frac{N_i}{en^2}B\ln(\varepsilon_\infty), \qquad (2)$$

where N_i is the density of scattering centers, n is the carrier density, v_F is the Fermi velocity at the Dirac cones, and ε_∞ is the high-frequency dielectric constant.[14,15] For electrons with conventional parabolic bands, $\triangle_{\rm LL} = \frac{e\hbar B}{m^*}$ and its evolution with field is very slow. Then, it is difficult to observe quantum limit and linear MR behavior in the moderate field range (below 9 T). Unusual linear magnetoresistance in the low-temperature range was identified in some materials hosting Dirac fermions with linear energy dispersion, such as $Ag_{2-\delta}(Te/Se)$, topological insulators, and $BaFe_2As_2$.[18–20,24,25] For Dirac states with linear energy dispersion, the energy splitting between the lowest and first LLs is described by $\triangle_{\rm LL} = \pm v_F\sqrt{2e\hbar B}$ where v_F is the Fermi velocity. It increases rapidly with field because of the large Fermi velocity

of Dirac fermions. Hence, in Dirac materials, the quantum limit and quantum transport can be achieved in the low-field region.

Large linear MR was also observed recently in $SrMnBi_2$. In $SrMnBi_2$, highly anisotropic Dirac states were identified where linear energy dispersion originates from the crossing of two Bi $6p_{x,y}$ bands in the double-sized Bi square nets. The crystal structure of $LaAgSb_2$ has quasi-two-dimensional Sb layers similar to the double-sized Bi square nets in $SrMnBi_2$. It could be expected that the Sb layers in $LaAgSb_2$ can also host Dirac fermions. The band structure in Fig. 1(d) shows two nearly linear narrow bands crossing the Fermi level along $Z-A$ and $\Gamma-M$ directions. The Fermi level is located very close to the Dirac-cone-like points. Quantum oscillation experiments revealed the hollow cylindrical Fermi surface in $LaAgSb_2$ and very small effective mass ($m^* \sim 0.16m_0$ where m_0 is the mass of the bare electron).[31,32] These results suggest that the unusual linear MR would originate from the quantum limit of Dirac fermions. Theoretical calculation predicted a very small pocket which has 20-T oscillation frequency and very small effective mass $\sim 0.06m_e$, although it was not observed in the experiment;[31] our first-principles results are consistent with this. These indicate possible small Dirac pockets in the system. Most likely, the quantum limit and linear MR are related to these very small pockets.

Taking the linear MR induced by the quantum limit into account and combing Eqs. (1) and (2), MR in $LaAgSb_2$ can be described very well by

$$\mathrm{MR} = \frac{\alpha B^2}{\beta + B^2} + \gamma |B|, \tag{3}$$

with α, β, γ as the fitting parameters.[10,14,26] The fitting curves for low temperature (<30 K) and higher temperature (>30 K) are shown in Figs. 3(a) and 4(a), respectively. Figure 3(b) gives the MR contribution from cyclotron motion and quantum linear MR at 2 K, respectively. The cyclotron MR contribution has very low saturation value ($\sim$0.03) and saturates at very small magnetic field ($\sim$0.4 T). The critical condition to achieve the quantum limit at finite temperature is $\Delta_{\mathrm{LL}} = E_F + k_B T$ and then the critical field B^* for Dirac fermions is $B^* = \frac{1}{2e\hbar v_F^2}(E_F + k_B T)^2$.[20] For conventional electron gas with parabolic bands, B^* is proportional to temperature. The temperature dependence of critical field B^* in $LaAgSb_2$ clearly deviates from the linear relationship and can be well fitted by $B^* = \frac{1}{2e\hbar v_F^2}(E_F + k_B T)^2$, as shown in Fig. 5(b). The fitting gives a large Fermi velocity $v_F \sim 1.46 \times 10^5$ ms^{-1}. The mobility of the system can be inferred from the semiclassical transport behavior in the low-field region. For a multiband system, the coefficient of the low-field semiclassical B^2 quadratic term A_2 is related to the effective electron and hole conductivity (σ_e, σ_h) and mobility (μ_e, μ_h) through $\sqrt{A_2} = \frac{\sqrt{\sigma_e \sigma_h}}{\sigma_e + \sigma_h}(\mu_e + \mu_h) = \mu_{\mathrm{MR}} = \sqrt{A_2}$, which is smaller than the average mobility of carriers $\mu_{ave} = \frac{\mu_e + \mu_h}{2}$ and gives an estimate of the lower bound to the latter.[20,24] Figure 5(b) shows the dependence of μ_{MR} on the temperature. At 2 K, the value of μ_{MR} is about 4000 cm^2/V s in $LaAgSb_2$, which is larger than the values in conventional metals and semiconductors. The parabolic temperature dependence of B^* and the large μ_{MR} confirm the existence of Dirac fermion states in $LaAgSb_2$. Another possible reason of the evolution of the crossover field B^* is the dependence of the carrier density and mobility. Although there is temperature evolution of the carrier density and mobility, Dirac fermions dominate the MR behavior and the large linear MR should be only due to the quantum limit of Dirac fermions. The temperature evolution of carriers should only influence the curve shape in the semiclassical transport region and the magnitude of the quantum linear MR since the quantum linear MR only depends on the Dirac fermions' density. In fact, the decrease of MR with temperature increasing should be attributed to the decrease of Dirac carriers. But, the crossover point from semiclassical transport region to quantum transport region should not be influenced by this temperature evolution of carrier density/mobility, but by the thermal fluctuation smearing out the LL splitting.

Another possibility for linear MR is the breakdown of weak-field magnetotransport at a simple density-wave quantum critical point.[33,34] Quasilinear MR was also found in Sr_2RuO_4 (Ref. 35) and $Ca_3Ru_2O_7$ (Ref. 33). Both of them are argued to be a small-gap-density wave system with quasi-2D Fermi surface. Theoretical analysis pointed out that at a simple density-wave quantum critical point, the weak-field regime of magnetotransport collapses to zero field with the size of the gap.[33,34] $LaAgSb_2$ also exhibits CDW transition at $\sim$200 K and the linear MR disappears around the CDW temperature. So, the linear MR or the Dirac fermions could be related to the CDW order. Similar phenomena were observed in $BaFe_2As_2$, in which the linear MR disappears above the spin density wave (SDW) temperature and the formation of Dirac fermions was attributed to the nodes of the SDW gap by complex zone folding in bands with different parities.[24,25] The detail mechanism of linear MR, the existence of Dirac fermion, as well as the relationship between Dirac fermions and CDW in $LaAgSb_2$ deserve further study using direct methods such as the angle-resolved photoemission spectroscopy (ARPES).

The magnetic field also has significant influence on the thermal transport of $LaAgSb_2$ [Figs. 2(b) and 2(c)]. Magnetic field suppresses thermal conductivity significantly below 200 K due to the large MR. Figures 6(a) and 6(b) show the magnetic field dependence of the Hall resistivity ρ_{xy} and Seebeck coefficient S at different temperatures, respectively. The behavior in ρ_{xy} is different from the classical Hall behavior. The positive ρ_{xy} are not linear in field but quadratic. The Hall resistivity curves all cross at $\sim$2 T. Below 2 T, ρ_{xy} increases with an increase in temperature, while it decreases with an increase in temperature above 2 T. This indicates the change in the apparent carrier density $n_{app} = B/(e\rho_{xy})$. Figure 6(c) shows the temperature dependence of n_{app} at several magnetic fields. At 2 K, the apparent carrier density at 1 T is reduced by a half in the 9-T field, implying the suppression of the DOS. This also induces the suppression of thermal conductivity in field (Fig. 2). More interestingly, n_{app} increases with an increase in temperature below 2 T, while it decreases with an increase in temperature for fields larger than 2 T. In the zero field, the Seebeck coefficient is negative in the whole temperature range. For magnetic field dependence of S [Fig. 6(b)], the absolute value decreases linearly with an increase in magnetic field below 2 T. It becomes zero at about 2 T when temperature is below 30 K. A further increase in field induces the changes of the sign of the Seebeck coefficient

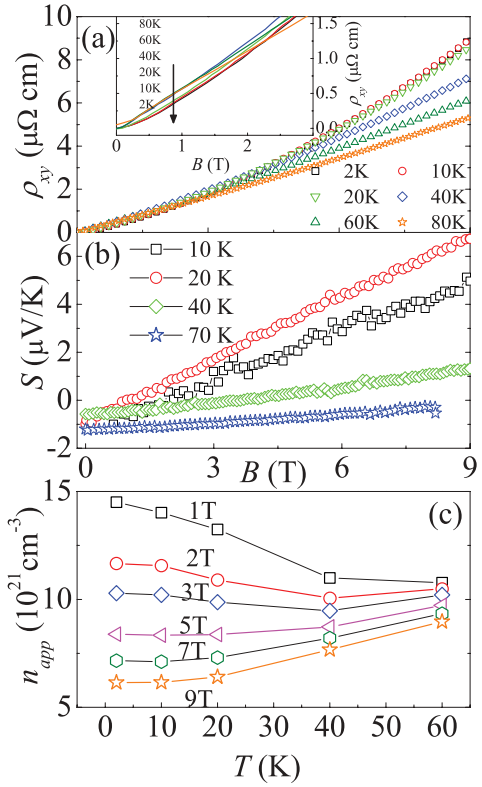

FIG. 6. (Color online) The magnetic field (B) dependence of the Hall resistivity ρ_{xy} (a) and Seebeck coefficient S (b) at different temperatures. Note the sign change at ~2 T in $S(B)$ at temperature below 70 K. The inset in (a) shows the Hall resistivity in field below 3 T. (c) The temperature dependence of the apparent carrier density as derived from Hall data in different fields.

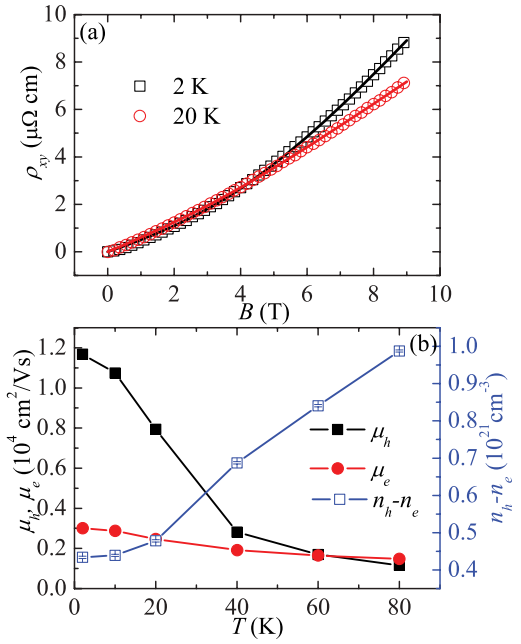

FIG. 7. (Color online) The fitting results for the magnetic field (B) dependence of the Hall resistivity ρ_{xy} at 2 and 20 K, respectively. (b) The temperature-dependent carrier mobility μ_h,μ_e and the carrier density ($n_h - n_e$) derived from the Hall resistivity fitting.

from negative to positive, and then the magnitude increases with an increase in field.

In a single-band metal with diffusion mechanism and electron-type carriers, the Seebeck coefficient is given by the Mott relationship

$$S = -\frac{\pi^2 k_B^2 T}{3e}\frac{\partial \ln \sigma(\mu)}{\partial \mu}, \tag{4}$$

where $\rho(\varepsilon)$ is the DOS, ε_F is the Fermi energy, k_B is the Boltzmann constant, and e is the absolute value of electronic charge.[36] The electron contribution to the Seebeck coefficient S_e is usually negative, while the hole contribution S_h is always positive.[36] For a two-band metal comprising electron and hole bands, S is expressed as

$$S = \frac{\sigma_h |S_h| - \sigma_e |S_e|}{\sigma_h + \sigma_e}, \tag{5}$$

where $\sigma_{e(h)}$ and $S_{e(h)}$ are the contributions of electrons (holes) to the electric conductivity and Seebeck coefficient, respectively. According to the classical expression for the Hall coefficient, including both electron- and hole-type carriers,[10,37]

$$\rho_{xy}/\mu_0 H = R_H = \frac{1}{e}\frac{\left(\mu_h^2 n_h - \mu_e^2 n_e\right) + (\mu_h\mu_e)^2(\mu_0 H)^2(n_h - n_e)}{(\mu_e n_h + \mu_h n_e)^2 + (\mu_h\mu_e)^2(\mu_0 H)^2(n_h - n_e)^2}, \tag{6}$$

where e is the electron charge, $n_{e(h)}$ and $\mu_{e(h)}$ represent the carrier concentrations and mobilities of the electrons (holes). Once there are two carrier types present, the field dependence of $\rho_{xy}(H)$ will become nonlinear. Moreover, Eq. (2) gives $R_H = \frac{1}{e}\frac{(\mu_h^2 n_h - \mu_e^2 n_e)}{(\mu_e n_h + \mu_h n_e)^2}$, when $\mu_0 H \to 0$, and $R_H = e^{-1} \cdot 1/(n_h - n_e)$ when $\mu_0 H \to \infty$.[37]

First-principles band structure in Fig. 1(c) shows that the Fermi level is located just below the Dirac-cone-like point of the gapless linear bands, but there is also a wide band crossing the Fermi level at the Z point. Most likely, the Dirac holes and the conventional electrons contribute to the transport simultaneously. The parabolic curves of ρ_{xy} plus the opposite signs between ρ_{xy} and $S(T)$ in the low field reflect the multiband effect. Hall resistivity ρ_{xy} can be fitted very well by the two-band Hall coefficient (6), as shown in Fig. 7(a) by two typical curves at 2 and 20 K. Combined with MR fitting using Eq. (1), we derive some parameters including carrier mobility (μ_h,μ_e) and carrier density $n = n_h - n_e$, as shown in Fig. 7(b). The holes have much higher mobility (~10^4 cm^2/V s) than the electrons at 2 K, and with increasing temperature, the hole mobility μ_h decreases significantly, but the change in the electron mobility μ_e is negligible. The value of mobility at 40 K derived from Hall resistivity is consistent with the magnitude from MR fitting. Moreover, the carrier density is positive, indicating the hole density is higher than the electron density.

Electronic transport in the Hall channel is determined by the density and mobility of different carriers, according to Eq. (6).[10] The Dirac holes have much higher mobility and dominate the Hall resistivity, which make ρ_{ab} of $LaAgSb_2$ positive. But, the Seebeck coefficient is proportional to the logarithmic derivative of the DOS at Fermi level and then

inversely proportional to the DOS at Fermi level or carrier density.[36] In particular, for the two-dimensional Dirac system with linear energy dispersion, $S \propto 1/\sqrt{n}$ could be expected and was indeed observed in graphene.[38,39] The electron density is smaller than the hole density according to the two-band analysis of Hall resistivity, and the electron band has smaller DOS in $LaAgSb_2$, so $|S_e|$ is larger than $|S_h|$ and in the zero-field, the Seebeck coefficient S is negative. With increasing magnetic field, the Dirac holes will occupy the zeroth LLs gradually and dominate the thermal transport behavior in the quantum limit since the Fermi level locates between the zeroth and first LLs and the DOS at the Fermi level is suppressed. The positive Hall resistivity and the Seebeck coefficient confirm the dominant holelike carriers in the high field, which induce the sign change in $S(B)$ at $\sim$2 T.

IV. CONCLUSION

In conclusion, we performed detailed magnetoresistance and magnetothermopower measurements in the $LaAgSb_2$ single crystal. The in-plane transverse magnetoresistance exhibits a crossover at a critical field B^* from the semiclassical weak-field B^2 dependence to the high-field linear-field dependence. The temperature dependence of B^* satisfies quadratic behavior. This, combined with the first-principles electronic structure, indicates the possible existence of Dirac fermions with linear energy dispersion. The linear magnetoresistance originates from the quantum limit of the possible Dirac fermions or the breakdown of weak-field magnetotransport at CDW transition. The Hall resistivity is positive, but the Seebeck coefficient is negative in the 0-T field. Analysis of Hall resistivity using the two-band model reveals that Dirac holes have higher mobility and larger density than conventional electrons, and dominate the electronic transport. Magnetic field suppresses the apparent Hall carrier density, and induces the sign change of the Seebeck coefficient from negative to positive. These effects are attributed to the magnetic field suppression of the density of states at Fermi level originating from the quantum limit of the Dirac holes.

ACKNOWLEDGMENTS

We than J. Warren for help with SEM measurements. Work at Brookhaven is supported by the US DOE under Contract No. DE-AC02-98CH10886.

[1] C. Song, Jaehyun Park, Japil Koo, K.-B. Lee, J. Y. Rhee, S. L. Bud'ko, P. C. Canfield, B. N. Harmon, and A. I. Goldman, Phys. Rev. B **68**, 035113 (2003).
[2] S. Guo, D. P. Young, P. W. Adams, X. S. Wu, J. Y. Chan, G. T. McCandless, and J. F. DiTusa, Phys. Rev. B **83**, 174520 (2011).
[3] S. L. Bud'ko, P. C. Canfield, C. H. Mielke, and A. H. Lacerda, Phys. Rev. B **57**, 13624 (1998).
[4] R. G. Goodrich, D. Browne, R. Kurtz, R. Young, J. F. DiTusa, P. W. Adams, and D. Hall, Phys. Rev. B **69**, 125114 (2004).
[5] D. P. Young, R. G. Goodrich, J. F. DiTusa, S. Guo, P. W. Adams, J. Y. Chan, and D. Hall, Appl. Phys. Lett. **82**, 3713 (2003).
[6] K. D. Myers, S. L. Bud'ko, I. R. Fisher, Z. Islam, H. Kleinke, A. H. Lacerda, and P. C. Canfield, J. Magn. Magn. Mater. **205**, 27 (1999).
[7] C. S. Lue, Y. F. Tao, K. M. Sivakumar, and Y. K. Kuo, J. Phys.: Condens. Matter **19**, 406230 (2007).
[8] L. Gondek, B. Penc, A. Szytula, and N. Stusser, J. Alloys Compd. **346**, 80 (2002).
[9] E. D. Mun, S. L. Bud'ko, and P. C. Canfield, J. Phys.: Condens. Matter. **23**, 476001 (2011).
[10] A. B. Pippard, *Magnetoresistance in Metals* (Cambridge University, Cambridge, England, 1989).
[11] J. Park, G. Lee, F. Wolff-Fabris, Y. Y. Koh, M. J. Eom, Y. K. Kim, M. A. Farhan, Y. J. Jo, C. Kim, J. H. Shim, and J. S. Kim, Phys. Rev. Lett. **107**, 126402 (2011).
[12] J. K. Wang, L. L. Zhao, Q. Yin, G. Kotliar, M. S. Kim, M. C. Aronson, and E. Morosan, Phys. Rev. B **84**, 064428 (2011).
[13] K. Wang, D. Graf, H. Lei, S. W. Tozer, and C. Petrovic, Phys. Rev. B **84**, 220401 (2011).
[14] A. A. Abrikosov, Phys. Rev. B **58**, 2788 (1998).
[15] A. A. Abrikosov, Europhys. Lett. **49**, 789 (2000).
[16] Y. Zhang, Z. Jiang, Y.-W. Tan, H. L. Stormer, and P. Kim, Nature (London) **438**, 201 (2005).
[17] D. Miller, K. Kubista, G. Rutter, M. Ruan, W. de Heer, P. First, and J. Stroscio, Science **324**, 924 (2009).
[18] D.-X. Qu, Y. S. Hor, J. Xiong, R. J. Cava, and N. P. Ong, Science **329**, 821 (2010).
[19] J. G. Analytis, R. D. McDonald, S. C. Riggs, J.-H. Chu, G. S. Boebinger, and I. R. Fisher, Nat. Phys. **6**, 960 (2010).
[20] A. A. Taskin, Z. Ren, S. Sasaki, K. Segawa, and Y. Ando, Phys. Rev. Lett. **107**, 016801 (2011).
[21] R. Xu, A. Husmann, T. F. Rosenbaum, M.-L. Saboung, J. E. Enderby, and P. B. Littlewood, Nature (London) **390**, 57 (1997).
[22] M. Lee, T. F. Rosenbaum, M.-L. Saboungi, and H. S. Schnyders, Phys. Rev. Lett. **88**, 066602 (2002).
[23] F. Y. Yang, K. Liu, D. H. Reich, P. C. Searson, and C. L. Chien, Science **284**, 1335 (1999).
[24] H.-H. Kuo, J.-H. Chu, S. C. Riggs, L. Yu, P. L. McMahon, K. DeGreve, Y. Yamamoto, J. G. Analytis, and I. R. Fisher, Phys. Rev. B **84**, 054540 (2011).
[25] K. K. Huynh, Y. Tanabe, and K. Tanigaki, Phys. Rev. Lett. **106**, 217004 (2011).
[26] I. Pallecchi, F. Bernardini, M. Tropeano, A. Palenzona, A. Martinelli, C. Ferdeghini, M. Vignolo, S. Massidda, and M. Putti, Phys. Rev. B **84**, 134524 (2011).
[27] M. Weinert, E. Wimmer, and A. J. Freeman, Phys. Rev. B **26**, 4571 (1982).
[28] P. Blaha, K. Schwarz, G. K. H. Madsen, D. Kvasnicka, and J. Luitz, WIEN2K, An Augmented Plane Wave + Local Orbitals Program for Calculating Crystal Properties (Karlheinz Schwarz, Techn. Universitat Wien, Austria).
[29] J. P. Perdew, K. Burke, and M. Ernzerhof, Phys. Rev. Lett. **77**, 3865 (1996).
[30] J. L. Olsen, *Electron Transport in Metals* (Interscience, New York, 1962).

[31]K. D. Myers, S. L. Bud′ko, V. P. Antropov, B. N. Harmon, P. C. Canfield, and A. H. Lacerda, Phys. Rev. B **60**, 13371 (1999).
[32]Y. Inada, A. Thamizhavel, H. Yamagami, T. Takeuchi, Y. Sawai, S. Ikeda, H. Shishido, T. Okubo, M. Yamada, K. Sugiyama, N. Nakamura, T. Yamamoto, K. Kindo, T. Ebihara, A. Galatanu, E. Yamamoto, R. Settai, and Y. Onuki, Philos. Mag. B **82**, 1867 (2002).
[33]J. Fenton and A. J. Schofield, Phys. Rev. Lett. **95**, 247201 (2005).
[34]A. J. Schofield and J. R. Cooper, Phys. Rev. B **62**, 10779 (2000).
[35]N. E. Hussey, A. P. Mackenzie, J. R. Cooper, Y. Maeno, S. Nishizaki, and T. Fujita, Phys. Rev. B **57**, 5505 (1998).
[36]R. D. Barnard, *Thermoelectricity in Metals and Alloys* (Taylor & Francis, London, 1972).
[37]R. A. Smith, *Semiconductors* (Cambridge University Press, Cambridge, England, 1978).
[38]P. Wei, W. Bao, Y. Pu, C. N. Lau, and J. Shi, Phys. Rev. Lett. **102**, 166808 (2009).
[39]Y. M. Zuev, W. Chang, and P. Kim, Phys. Rev. Lett. **102**, 096807 (2009).